Available online at www.sciencedirect.com

ScienceDirect

Procedia Structural Integrity 28 (2020) 1329–1339

Structural Integrity Procedia

www.elsevier.com/locate/procedia

1st Virtual European Conference on Fracture

Fatigue Strength Evaluation of Notched Ductile Steel Specimens Using Critical Distances

Bruno Atzori*, Mauro Ricotta, Alberto Campagnolo, Daniele Rigon, Giovanni Meneghetti

Department of Industrial Engineering, via Venezia, 1, 35131, Padova, Italy

Abstract

In the case of AISI 304L austenitic stainless steel it was found that the fatigue strength of specimens characterized by the presence of blunt notches cannot be rationalized either in terms of linear elastic local stress or nominal stress amplitude. This fact was related to the high level of ductility shown by this material also in the case of high cycle fatigue regime. Therefore, in this paper some classical fatigue design methodologies are extended to account for this aspect also in the case of severe notches. On this basis a FEM oriented extension of the concept of geometric elastic stress concentration factor is proposed.

Keywords: Crtical distances, ductility, fatigue, severe notches, AISI 304L

1. Introduction

In a previous work, Meneghetti et al (2013), it was shown that in the case of AISI 304L stainless steel, neither net-section nor linear elastic peak stresses are able to rationalise in a single scatter curve the fatigue life of bluntly notched specimens. On the contrary, it was successfully synthesised in a single scatter band, by considering the dissipated heat energy density per cycle (the Q parameter) as fatigue damage indicator.

Recently Atzori et al (2018) pointed out that, concerning the plain specimens tested in Meneghetti et al (2013), at the fatigue knee the plastic strain energy density was 1.49 times higher than the elastic strain energy density. The

* Corresponding author. Tel.: +39 049 827 6762; fax: +39 049 827 6785.
E-mail address: bruno.atzori@unipd.it

10.1016/j.prostr.2020.10.104

authors stated that the presence of plasticity at the fatigue knee was responsible for the unsuitableness of classical stress-based approaches to synthesise the fatigue behaviour of this material. On the contrary, the elastic-plastic strain energy density was found an efficient parameter to rationalise in a single scatter band fatigue data of plain and bluntly notched specimens. Based on this result, the classic stress- and the point stress-based approaches were revisited taking into account the presence of plasticity at the fatigue knee, by introducing an equivalent fully elastic material having a linear elastic strain energy density at the fatigue knee, equal to that of the actual material. Accordingly, a coefficient of plasticity, K_p, was successfully introduced to modify the classical definition of fatigue strength reduction factor, K_f.

In this work, the analysis is extended to the case of severe notches. After recalled the theoretical reasons that underlie the differences in behaviour caused by the ductility, some of the most widespread methodologies used today are analysed and discussed: the classic one, based on the stress concentration factor and the notch sensitivity index, and the critical distances, applied through the point stress criterion.

As a result, it is seen that the classical approach and the point stress criterion can be applied also in the case of ductile materials.

Nomenclature

K'	material cyclic strength coefficient [MPa]
K_f	fatigue notch factor
$K_{fn,p}$	fatigue notch factor in the presence of plasticity at the fatigue limit
K_p	coefficient of plasticity
K_{tn}	theoretical stress concentration factor referred to the net-section
$K_{tn,point}$	geometric linear elastic stress concentration factor referred to the net-section
q	notch sensitivity index
r_n	notch radius [mm]
R_p	plasticity ratio
n'	cyclic hardening exponent
N_0	number of cycles at fatigue limit for plain material
N_{th}	number of cycles at threshold for mode I crack propagation
x(N)	critical distance evaluated at N number of cycles [mm]
$x(N_0)$	critical distance evaluated at N_0 [mm]
x_0	critical distance evaluated at N_{th} [mm]
$W_{LE}(\sigma_0)$	elastic strain energy density evaluated at the fatigue limit [MJ/m^3]
$W_{CC}(\sigma_0)$	elastic-plastic strain energy density at the fatigue limit [MJ/m^3]
$W_{CC}^E(\sigma_0)$	elastic component of $W_{CC}(\sigma_0)$ [MJ/m^3]
$W_{CC}^P(\sigma_0)$	plastic component of $W_{CC}(\sigma_0)$ [MJ/m^3]
ε_0^E	elastic component of the strain evaluated at the fatigue limit
ε_0^P	plastic component of the strain evaluated at the fatigue limit
σ_0, $\Delta\sigma_0$	material fatigue limit, its range [MPa]
$\Delta\sigma_{0n}$	range of the fatigue limit of notched material [MPa]

2. Theoretical background

In Atzori et al (2018), the elastic-plastic Strain Energy Density (SED) is assumed the damage variable able to correlate the fatigue strength of plain and notched components. The underlying concept is that two components have the same fatigue life when they have the same level of elastic-plastic SED.

Usually at the fatigue knee, the plain material behaviour is supposed to be elastic and consequently the relevant strain energy density is equal to the elastic strain energy density, W_{LE}

$$W_{LE}(\sigma_0) = \frac{\sigma_0^2}{2 \cdot E} \tag{1}$$

being σ_0 the material fatigue limit and E its elastic modulus.

Nevertheless, when at the fatigue knee plasticity can not be neglected, the relevant elastic-plastic SED can be calculated according to Eq. 2:

$$W_{CC}(\sigma_0) = W_{CC}^E(\sigma_0) + W_{CC}^P(\sigma_0) \tag{2}$$

where $W_{CC}^E(\sigma_0)$ and $W_{CC}^P(\sigma_0)$ is the elastic and the plastic component of $W_{CC}(\sigma_0)$, respectively. The material cyclic behaviour can be described by the Ramberg-Osgood law, according to which the strain is the sum of its elastic, ε^E, and its plastic component, ε^P, as follows:

$$\varepsilon = \varepsilon^E + \varepsilon^P = \frac{\sigma}{E} + \left(\frac{\sigma}{K'}\right)^{\frac{1}{n'}} \tag{3}$$

where K' is the cyclic strength coefficient and n' the cyclic hardening exponent. Therefore, it can be derived that:

$$W_{CC}^E(\sigma_0) = \frac{1}{2}\sigma_0 \cdot \varepsilon_0^E = \frac{\sigma_0^2}{2E} \tag{4a}$$

$$W_{CC}^P(\sigma_0) = \frac{1}{1+n'} \cdot \sigma_0 \cdot \varepsilon_0^P = \frac{1}{1+n'} \cdot \sigma_0 \cdot \left(\frac{\sigma_0}{K'}\right)^{\frac{1}{n'}} \tag{4b}$$

ε_0^E and ε_0^P being the elastic and the plastic component of the strain at the fatigue knee, respectively. Therefore, the high cycle fatigue strength assessment of bluntly notched components can be performed by comparing the elastic-plastic SED, evaluated at the notch root, to the elastic-plastic SED of plain material.

Usually, at the fatigue limit the behaviour of plain material is supposed to be fully elastic. To overcome this limitation, in Atzori et al (2018), an equivalent fatigue limit $\sigma_{0,eq}$ was introduced (see Fig.1a) such that the SED experimentally measured at the fatigue knee for plain material is equal to that of an equivalent fully elastic plain material, following the original idea proposed by Molski and Glinka (1981) and Glinka (1985), regarding notched components:

$$W_{LE}(\sigma_{0,eq}) = W_{CC}(\sigma_0) = W_{CC}^E(\sigma_0) + W_{CC}^P(\sigma_0) \tag{5}$$

where $W_{LE}(\sigma_{0,eq}) = \frac{\sigma_{0,eq}^2}{2 \cdot E}$.

Then in Atzori et al (2018), a coefficient of plasticity K_p, was defined as follows:

$$K_p = \frac{\sigma_{0,eq}}{\sigma_0} = \sqrt{\frac{W_{LE}(\sigma_{0,eq})}{W_{SCC}^E(\sigma_0)}} = \sqrt{1 + \frac{2}{1+n'} \cdot R_p} \tag{6a}$$

being $R_p = \varepsilon_0^P / \varepsilon_0^E$ the plasticity ratio evaluated at the fatigue limit. The K_p coefficient versus R_p of plain material is plotted in Fig. 1b for different values of n'. Other approaches are available in literature to correlate elastic-plastic to linear elastic analyses. Of these, Neuber's rule is the most widely used and the relevant K_p versus R_p trend is plotted in the same figure, according to Eq. 6b

$$K_p^N = \sqrt{1 + R_p} \tag{6b}$$

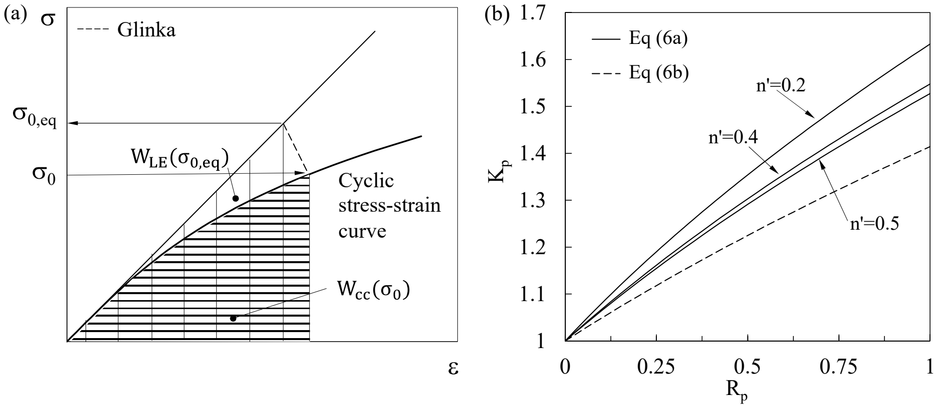

Fig. 1. a) schematic view of equivalent fatigue limit concept and b) K_p versus R_p trend for different values of cyclic hardening exponent.

2.1. Nominal stress approach

The nominal stress approach assumes that a notched component reaches the fatigue knee when an effective stress acting at the notch tip, σ_{eff}, is equal to the fatigue limit of plain material. Usually, σ_{eff} is evaluated by starting from the evaluation of a nominal stress σ_{nom} properly increased by using the fatigue notch factor K_f (Peterson (1959)).

In general, K_f is an experimental parameter defined as:

$$K_f = \frac{\text{fatigue limit of unnotched specimen}}{\text{fatigue limit of notched specimen}} \tag{7}$$

It is well known that when the K_f value is not available, it can be estimated by starting from the theoretical stress concentration factor K_t and the notch sensitivity index q, according to Peterson (1959):

$$q = \frac{K_f - 1}{K_t - 1} \tag{8}$$

The values of q vary from q=0 for no notch effect (K_f=0) to q= 1 for the full theoretical effect (K_f=K_t). Therefore, in Atzori et al (2018), the classical approach was extended to materials characterised by plasticity at the fatigue knee, by imposing that a notched component reaches the fatigue knee when the effective stress σ_{eff} is equal to $\sigma_{0,eq}$.

In the case of full theoretical effect q=1 (i.e. K_f=K_t) and by using the net-section stress as nominal stress, it follows:

$$\sigma_{eff} = \sigma_{0,eq} \Rightarrow K_{tn} \cdot \sigma_{0,net} = K_p \cdot \sigma_0 \tag{9}$$

where $\sigma_{0,net}$ is the nominal stress to be applied to the notched component to reach the fatigue knee. Therefore, a new strength reduction factor can be defined which considers for the plasticity of plain material at the fatigue knee:

$$K_{fn,p} = \frac{K_{tn}}{K_p} \tag{10}$$

Eq. 10 being valid when $K_{tn} > K_p$. On the contrary, $K_{fn,p}$=1 when $K_p < K_{tn}$, since in this case one can suppose that the fatigue knee of notched component is equal to that of plain material. When a partial theoretical effect is considered (i.e $0 < q < 1$):

$$K_{fn,p} = \frac{1 + q \cdot (K_{tn} - 1)}{K_p} \tag{11}$$

Finally, once the fatigue knee of notched component was defined, the S-N curve was completely evaluated, assuming that in the low cycle fatigue regime the notch effect vanishes, thanks to the diffuse plasticity, that can completely involve the net-section. Usually, in the classical nominal stress approach the stress-life curve is defined for a number of cycles to failure starting from 1000 cycles (e. g Dowling (2013)). In view of this, in Atzori et al (2181) it was assumed that the fatigue strength of notched component is equal to that of the plain material evaluated at N=1000 cycles.

2.2. Point stress approach

Concerning the evaluation of the fatigue strength of cracked components, Linear Elastic Fracture Mechanics (LEFM) concepts can be adopted. The underlying idea is that the range of the mode I stress intensity factor ΔK_I, evaluated by means of linear elastic finite element analyses, has to be compared to the threshold range value of the mode I stress intensity factor, ΔK_{th}, as follows:

$$\Delta K_I < \Delta K_{th} \tag{12}$$

In this case, ΔK_I and ΔK_{th} are evaluated under the hypothesis of linear elastic material behaviour and then the influence of plasticity is considered implicitly. The LEFM-based approach was extended to severe notches (see Tanaka (1983), Taylor (1999) and Atzori et al (2003), as examples).

Let us consider the case of a severe notch with notch opening angle equal to zero. Once the stress field trend controlled by the notch radius has been exceeded (the extension of which has been estimated to be 20% of the notch radius in Atzori et al (2003)), the stress field will have a similar trend to that due to a crack, as follows:

$$\Delta\sigma_y = \frac{\Delta K}{\sqrt{2\pi x}} \tag{13}$$

Therefore, through Eq.(13), Eq.(12) can be extended to severely notched components at the fatigue limit.

Usually, concerning the severe notches, the fatigue strength is evaluated considering the stress range acting at a critical distance x_0 from the notch tip. From Eq.(13):

$$x_0 = \frac{1}{2\pi}\left(\frac{\Delta K_{th}}{\Delta\sigma_0}\right)^2 \tag{14}$$

where σ_0 is the fatigue limit of the plain material. The fatigue strength of severe notch is then expressed in terms of the stress range evaluated at x_0, instead of the nominal stress range. Eq.(14) can be generalised, as follows:

$$x(N) = \frac{1}{2\pi}\left(\frac{\Delta K(N)}{\Delta\sigma(N)}\right)^2 \tag{15}$$

Eq.(15) is particularly useful when the fatigue curves of plain and cracked material have different knee-points as schematically reported in Fig.2, where the classical application of the point stress approach is represented by light-blue line, while the green line shows the point stress approach applied considering the fatigue limit of the plain material, N_0

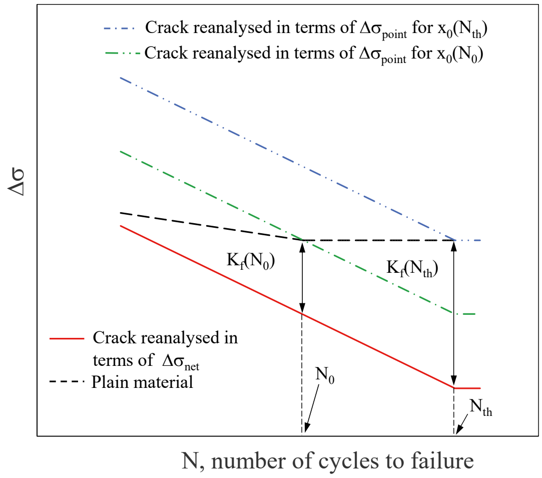

Fig. 2. Comparison between the fatigue curves of plain and cracked material in terms of the net-stress range and the point stress range evaluated at $x(N_0)$ and $x(N_{th})$.

To easily forward the point stress approach to severe notches, it is useful to define the point stress concentration factor as follows:

$$K_{tn,point}(x(N)) = \frac{\sigma_{yy}(x(N))}{\sigma_{net}} \tag{16}$$

that depends on the critical distance evaluated according to Eq.(15).

The extended point stress approach will be applied to specimens made by ductile AISI 304L stainless-steel weakened by severe notches in the next section.

3. Material and experimental results

The theoretical approaches presented in this paper were applied to experimental results obtained by carrying out stress and strain-controlled fatigue tests on 4-mm-thick AISI 304L stainless steel specimens. The determination of the cyclic curve of the material was made with a limited number of tests, since the results obtained proved to be in excellent agreement with those obtained from a previous batch of the same material published in Meneghetti et al (2013). Mechanical properties are listed in Table 1, with the cyclic parameters of Ramberg-Osgood curve:

$$\varepsilon = \frac{\Delta\varepsilon^E}{2} + \frac{\Delta\varepsilon^P}{2} = \frac{\sigma}{E} + \left(\frac{\sigma}{K'}\right)^{\frac{1}{n'}} \tag{17}$$

Table 1. Mechanical properties of AISI 304L stainless-steel (from Meneghetti et al (2013) and Rigon et al (2017))

	E [MPa]	$R_{p0.2}$ [MPa]	R_m [MPa]	K' [MPa]	n'	$\Delta\sigma_0$ [MPa]	N_0 [cycles]	K_p	ΔK_{th} [MPa·√m]
1st batch	194700	327	690	4083	0.433	450	160000	1.57	/
2nd batch	194700	279	620	4083	0.433	404	160000	1.52	8.69

The values of ε_0^E and ε_0^P relevant to 6-mm-thick sheets were calculated in Atzori et al (2018) giving Rp=1.57 (see Eq.(6a), while those relevant to 4-mm-thick were found equal to the Rp=1.52.

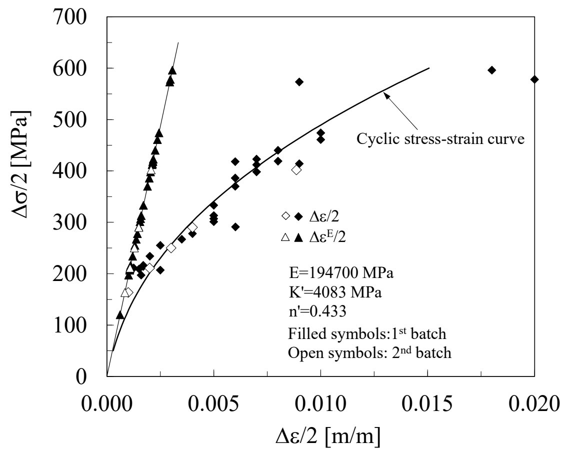

Fig.3. Cyclic stress-strain curve of AISI 304L stainless steel (strain-controlled fatigue tests).

This paper refers to the second batch of material. Axial, zero-mean stress fatigue tests were carried out on specimens with the geometry reported in Rigon et al (2017) and Meneghetti et al (2016). For ease of reading, here it is recalled that samples had notch opening angle $2\alpha=45°$ and 135° and notch radius equal to $r_n=3$, 1 and 0.5 mm. The K_{tn} values, referred to the net section are listed in Table 2 with the reference fatigue strength evaluated at 160000 cycles, $\Delta\sigma_{0n}$, and the experimental values of fatigue notch factor, $K_{f,sper}(N_0) = \Delta\sigma_0/\Delta\sigma_{0n}$. The experimental results are shown in Fig. 4.

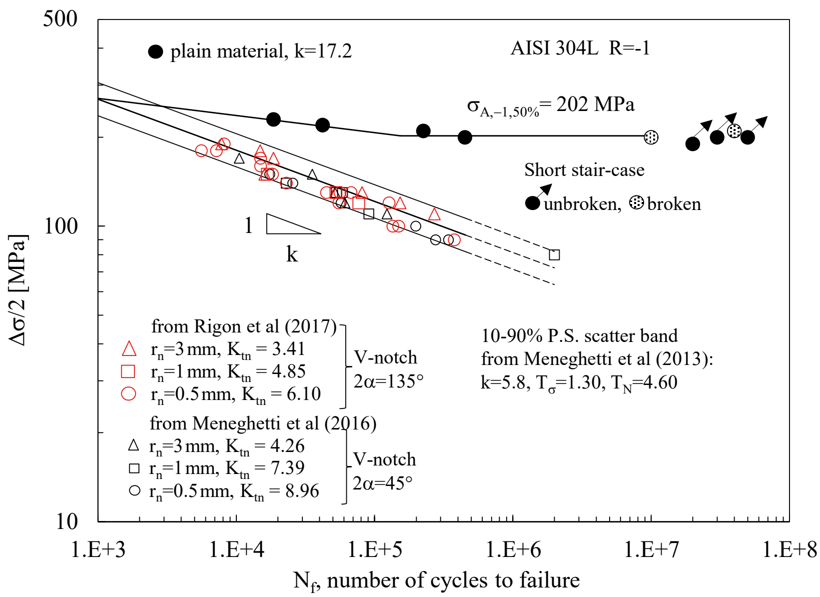

Fig. 4. Fatigue data of AISI 304L plain and notched specimens (2nd batch).

3.1. Experimental results reanalyzed according to the nominal stress approach

The nominal stress approach was applied to the experimental data plotted in Fig.4 and the results are listed in Table 2. One can see that the difference between theoretical and experimental values increases as the notch tip radius decreases, although the effect of ductility was taken into account by means of the K_p coefficient. Considering the significant difference observed in terms of number of cycles between the plain material and the geometry having the smallest notch radius (r_n=0.1 mm, Table 2), it can be supposed that N_{0n} increases, as the notch tip decreases. This hypothesis was not experimentally verified yet, but fatigue tests will be carried in the next future. By assuming that the $\Delta\sigma_{0n}$ values are correct, the fatigue curves of notched specimens were calculated, by evaluating the number of cycles N_{0n}, listed in Table 2.

Table 2. Experimental results plotted in Fig.4 reanalysed according to the nominal stress approach

2α [°]	r_n [mm]	$\Delta\sigma_n(N_0)^*$ [MPa]	$K_f(N_0)$	K_{tn}	q	K_f	$K_{f,p}=\frac{K_f}{K_p}$	$\Delta\sigma_{0n}=\frac{\Delta\sigma_0}{K_{f,p}}$ [MPa]	N_{0n} [cycles]	$R_n=\frac{N_{0n}}{N_0}$
45	3	222.0	1.82	4.26	0.93	4.03	2.65	152.4	$1.40\cdot10^6$	8.9
	1	208.2	1.94	7.39	0.82	6.24	4.11	98.2	$12.5\cdot10^6$	78.2
	0.5	209.3	1.93	8.96	0.69	6.49	4.27	94.6	$16.0\cdot10^6$	100.3
45÷90	0.1	181.6	2.22	26.6	0.31	8.94	5.88	68.8	$28.0\cdot10^6$	175.0
135	3	222.0	1.82	3.41	0.93	3.24	2.13	189.6	$0.40\cdot10^6$	2.5
	1	208.2	1.94	4.85	0.82	4.16	2.74	147.4	$1.20\cdot10^6$	7.4
	0.5	209.3	1.93	6.10	0.69	4.52	2.97	136.0	$2.00\cdot10^6$	12.2

*Experimental results

3.2. Experimental results reanalyzed according to the point stress approach

Fig. 5 shows the fatigue curve of plain and cracked material (Meneghetti et al (2016)). The latter was reanalyzed in term of ΔK as well as $\Delta\sigma_n$ and one can see the significant difference between N_0 and N_{th}, supporting the hypothesis that the number of cycles corresponding to the fatigue limit increases, as the notch tip radius decreases. Therefore, from Eq.(15) different critical distances can be calculated:

$$x_0 = x(N_{th}) = \frac{1}{2\pi}\left(\frac{\Delta K_{th}}{\Delta\sigma_0}\right)^2 = \frac{1}{2\pi}\left(\frac{8.69}{404}\right)^2 \text{ [m]} = 0.074 \text{ [mm]} \quad (18)$$

$$x(N_0) = \frac{1}{2\pi}\left(\frac{\Delta K(N_0)}{\Delta\sigma_0}\right)^2 = \frac{1}{2\pi}\left(\frac{28.8}{404}\right)^2 \text{ [m]} = 0.81 \text{ [mm]} \quad (19)$$

The linear elastic stress fields, obtained by finite element analyses by imposing σ_{net}=1 MPa, are shown in Fig.6, where for completeness of information the blunt notches obtained by the 1st batch of material are reported. Table 3 summarises the $K_{t,point}$ values (see Eq.(16)), relevant to the critical distances evaluated by Eq.(18) and Eq.(19).

Fig.6 shows that for the critical distance $x(N_0)$, the stress field of notched geometries is comparable to that of a crack having the length equal to the notch depth, while for $x(N_{th})$ the stress field is controlled by the geometry of the notch tip.

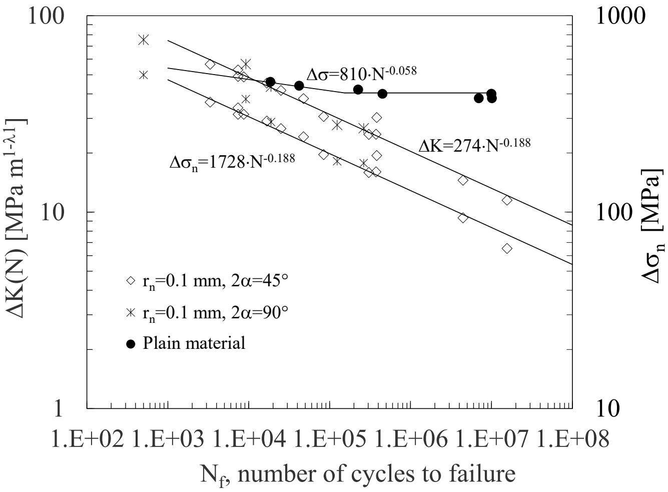

Fig.5 Fatigue curves of plain and cracked AISI 304L stainless steel (2nd batch).

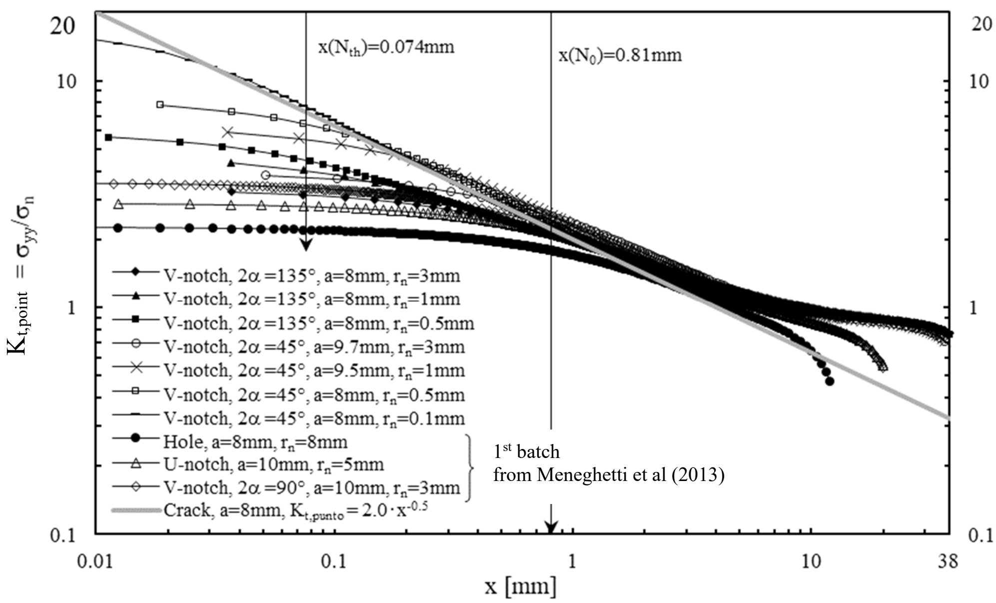

Fig. 6. Linear elastic stress fields evaluated by finite element analyses for the different analysed specimen geometries.

Therefore the $\Delta\sigma_{0n}$ values were calculated, according to Eq.(20):

$$\Delta\sigma_n(N_0) = \frac{\Delta\sigma_0}{K_{t,point}(x(N_0))} \tag{20}$$

and the results are summarised in Table 3. It is worth noting that for x= $x(N_0)$, the influence of plasticity was not taken into account because the stress was picked up at $x(N_0)$ where the stress field is close to that of a the equivalent crack, while for x= $x(N_{th})$, the K_p coefficient was used:

$$K_{f,p} = \frac{K_{t,point}(x(N_{th}))}{K_p} \tag{21}$$

therefore

$$\Delta\sigma_{0n} = \frac{\Delta\sigma_0}{K_{f,p}} \tag{22}$$

Table 3. Experimental results plotted in Fig.4 reanalysed according to the point stress approach

2α [°]	r_n [mm]	$\Delta\sigma_n(N_0)^*$ [MPa]	$K_{t,point}(N_0)$	$\Delta\sigma_n(N_0)^\circ$ [MPa]	$K_{t,point}(N_{th})$	$K_{f,p}$	$\Delta\sigma_{0n}^{\circ\circ}$ [MPa]	N_{0n} [cycles]	$R_n = N_{0n}/N_0$
45	3	222.0	2.41	167.6	3.59	2.36	171.0	$0.72\cdot10^6$	4.5
	1	208.2	2.42	166.9	5.36	3.53	114.6	$5.1\cdot10^6$	31.9
	0.5	209.3	2.36	171.1	6.43	4.23	95.5	$15.3\cdot10^6$	95.5
45÷90	0.1	181.6	2.22	182.0	7.37#	7.37#	54.8	$93.8\cdot10^6$	586.2
135	3	222.0	2.13	189.7	3.14	2.07	195.6	$0.40\cdot10^6$	2.1
	1	208.2	2.10	192.4	3.90	2.57	157.5	$0.81\cdot10^6$	5.0
	0.5	209.3	2.08	194.2	4.45	2.93	138.0	$1.8\cdot10^6$	11.3

* experimental values; ° from Eq.(20); °° from Eq.(22); # plasticity was not considered

One can see that the $\Delta\sigma_n(N_0)$ values are lower than the relevant experimental data and that, as it can be expected, the estimated results are closer to the experimental values, the smaller the notch radius.

4. Conclusions

In this paper, the fatigue strength evaluation of ductile severely notched specimens using the nominal stress and the point stress approaches is addressed. In more detail, a theoretical model previously developed by the authors for the fatigue life assessment of ductile specimens weakened by blunt notches was extended. The fundamental concept is that a ductile plain specimen can experience plastic deformations at the fatigue limit. In view of this, a coefficient of plasticity K_p was introduced, which assured that the elastic-plastic strain energy density evaluated at the fatigue knee is maintained. Once the K_p parameter was defined, the nominal stress approach was modified.

Concerning the point stress approach, the concept of geometric linear elastic stress concentration factor was introduced and the definition of critical distance was generalised by introducing the dependence on the number of cycles. In fact, the number of cycles at the fatigue limit of plain material can be different with respect to that for the threshold of crack propagation.

The theoretical approaches were then applied to evaluate the fatigue strength of 4-mm-thick, hot-rolled AISI 304 L stainless specimens, weakened by severe notches, having radius equal to 3, 1 and 0.5 mm, starting from the fatigue curve of plain material.

Considering the preliminary results published in this paper, a good correlation was found between the experimental and the calculated fatigue strength of notched specimens.

References

Atzori, B., Lazzarin, P., Meneghetti, G., 2003. Fracture mechanics and notch sensitivity. Fatigue & Fracture of Engineering Materials & Structures, 26, 257–67.

Atzori, B., Ricotta, M., Meneghetti, G., 2018. Strain energy-and stress-based approaches revisited in notch fatigue of ductile steels, Fatigue2018, MATEC Web of Conferences 165, paper #14009.

Dowling, N.E., 2013, "*Mechanical behaviour of materials*", Pearson Prentice Hall.

Glinka, G., 1985. Calculation of inelastic notch-tip strain-stress histories under cyclic loading", Engineering Fracture Mechanics, 22, 839-854.

Meneghetti, G., Ricotta, M., Atzori, B., 2013. A synthesis of the push-pull fatigue behaviour of plain and notched stainless-steel specimens by using the specific heat loss. Fatigue & Fracture of Engineering Materials & Structures, 36, 1306-1322.

Meneghetti, G., Ricotta, M., Atzori, B., 2016. The heat energy dissipated in a control volume to correlate the fatigue strength of bluntly and severely notched stainless-steel specimens, Proceedings of the 21st European Conference on Fracture, ECF21. Catania, Italy, vol. 2, pp. 2076–2083.

Molski, K., Glinka, G., 1981. A method of elastic-plastic stress and strain calculation at a notch root. Materials Science and Engineering, 50, 93-100.

Peterson, R.E., 1959. Notch sensitivity, in "*Metal fatigue*". In: Sines, G. Waisman, JL. (Ed.). New York: MacGraw-Hill;. p. 293–306.

Rigon, D., Ricotta, M., Meneghetti, G., 2017. An analysis of the specific heat loss at the tip of severely notched stainless steel specimens to correlate the fatigue strength. Theoretical and Applied Fracture Mechanics, 92, 240–251.

Tanaka, K., 1983. Engineering formulae for fatigue strength reduction due to crack-like notches. International Journal of Fracture, 22, R39-R46.

Taylor, D., 1999. Geometrical effects in fatigue: a unifying theoretical model. International Journal of Fatigue, 21, 413-420.